LA-8694-MS

Location Capability of the Los Alamos National Laboratory Seismic Array, Northern New Mexico

University of California

LOS ALAMOS SCIENTIFIC LABORATORY
Post Office Box 1663 Los Alamos, New Mexico 87545

This report was not edited by the Technical Information staff.

UNITED STATES
DEPARTMENT OF ENERGY
CONTRACT W-7405-ENG. 36

Printed in the United States of America
Available from
National Technical Information Service
US Department of Commerce
5285 Port Royal Road
Springfield, VA 22161

Microfiche $3.50 (A01)

Page Range	Domestic Price	NTIS Price Code	Page Range	Domestic Price	NTIS Price Code	Page Range	Domestic Price	NTIS Price Code	Page Range	Domestic Price	NTIS Price Code
001-025	$ 5.00	A02	151-175	$11.00	A08	301-325	$17.00	A14	451-475	$23.00	A20
026-050	6.00	A03	176-200	12.00	A09	326-350	18.00	A15	476-500	24.00	A21
051-075	7.00	A04	201-225	13.00	A10	351-375	19.00	A16	501-525	25.00	A22
076-100	8.00	A05	226-250	14.00	A11	376-400	20.00	A17	526-550	26.00	A23
101-125	9.00	A06	251-275	15.00	A12	401-425	21.00	A18	551-575	27.00	A24
126-150	10.00	A07	276-300	16.00	A13	426-450	22.00	A19	576-600	28.00	A25
									601-up	†	A99

†Add $1 00 for each additional 25-page increment or portion thereof from 601 pages up.

LA-8694-MS

UC-11
Issued: February 1981

Location Capability of the Los Alamos National Laboratory Seismic Array, Northern New Mexico

D. J. Wechsler

LOCATION CAPABILITY OF THE LOS ALAMOS NATIONAL LABORATORY SEISMIC ARRAY, NORTHERN NEW MEXICO

by

D. J. Wechsler

ABSTRACT

The adequacy of the Los Alamos National Laboratory seismic array in northern New Mexico has been evaluated by a recently implemented least squares inversion program for seismic arrival time data. The condition number of the partial derivative matrix of travel times provides information for estimating the quality of hypocentral solutions. Spatial variation of the condition number combined with the results of inversion of synthetic arrival time data enables us to assess the capability of the seismic array in locating earthquakes occurring throughout the northern part of the state. The results define a large portion of north-central New Mexico over which earthquake epicenters can be detected and located by the Los Alamos array.

I. INTRODUCTION

Regional and local seismicity studies require quantitative estimates of the precision of seismic event location. The precision of an earthquake hypocenter location determined using present computer algorithms is affected by two factors: the computer algorithm itself and the station geometry or array configuration. The Los Alamos National Laboratory has monitored the seismic activity in northern New Mexico since 1973. The number of stations in the Los Alamos array has increased in later years (1976-1980) to the present network of 24 permanent stations (Table I). In 1980 a new computer location code was adapted for use with the seismic arrival-time data, and concurrently an investigation into the improvement of locations and the effects of some inadequacies in station coverage was completed. The results of the study indicate optimum areas for future array expansion and also give some insight into the weaknesses of the location codes.

II. COMPUTER LOCATION CODES

A. Description of Codes

Until January of 1980 all earthquakes were located using a computer code written by J. Stewart of Los Alamos based on the method of intersecting spherical wavefronts. That program computes wavefront radii using a single velocity estimate, either 6 or 8 km/sec depending on whether the first P-wave arrival was determined to be a refracted phase from the crustal basement (Pg) or the mantle (Pn). Origin times are estimated using the ratio of P to S arrivals, assuming a Poisson's ratio of 0.25. The program then uses an arithmetic mean of each triple intersection to obtain values for latitude, longitude, and depth.

The computer code now being used for earthquake hypocenter determination is a modified version of HYPOINVERSE (Klein, 1978). The algorithm is based on a least squares minimization of the travel time residuals, but solves the partial derivative matrix of parameters (latitude, longitude, depth, and origin time) by a method of generalized inversion. For a more complete discussion of the theory and computational method see Klein (1978) and Lee and Lahr (1975).

There are several advantages in using this program rather than the sphere program described above. Perhaps the most obvious is the option to use three different layered velocity models or travel-time tables simultaneously, with or without station delays. Thus we can now take advantage of the information obtained from crustal refraction profiles in the region (Olsen et al., 1979, Toppozada and Sanford, 1976, Roller, 1965). A second advantage is the ability to obtain an estimate of origin time without depending on S-arrivals, although a good S-arrival is thought to improve the estimate. Constraining the depth parameter to some reasonable number is often desirable because the focal depth often cannot be adequately resolved. A large error in depth will in turn bias the earthquake epicenter, so the option to constrain the depth is often employed. Another useful option in the HYPOINVERSE code is the ability to assign weights to stations of varying quality before an attempt is made to determine a location.

B. Evaluating Hypocenter Locations

A major consideration in choosing the HYPOINVERSE code to adapt to the Los Alamos system was the statistical information obtainable from the inversion. This information can give a more quantitative and immediate indication

of the precision of the solution and the adequacy of and errors in the data. Klein (1978) has given a summary of the inverson scheme and an explanation of the results, so I will only briefly describe a few of the considerations made in judging the quality of the solutions.

The value of the root mean square (RMS) of the travel-time residuals, gives an indication of the amount of noise in the data. Other useful information provided by HYPOINVERSE is the orientation of the error ellipsoid, the form of the parameter covariance matrix, and station importance factors (computed from the information density matrix). A further useful result can be obtained by a simple computation of the condition number of the partial derivative matrix (A) of parameters. This feature was added to the HYPOINVERSE code, and makes use of the fact that the eigenvalues are retained from the inversion algorithm. The condition number as used here is the ratio of the largest to the smallest eigenvalue and is a measure of the numerical stability of the problem. The condition number can also reflect the effects of seismic array geometry on the stability of the problem. In Figs. 1-11, each point represents a value for an earthquake located in northern New Mexico. A total of 233 events was used. Figure 1 depicts a linear relationship between the maximum azimuthal gap (using event to station azimuths) and the log of the condition number. This indicates that the location problem for an event outside the array becomes numerically unstable and will have a large condition number.

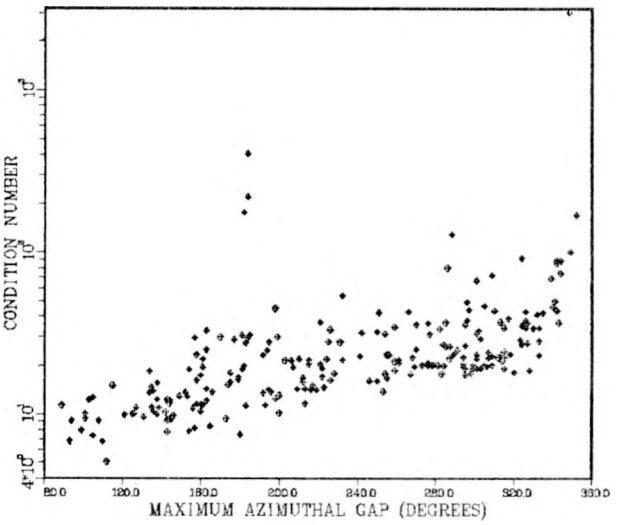

Fig. 1
Condition number of partial derivative matrix (A) plotted against maximum azimuthal gap between recording stations for 233 events.

There is also evidently a relationship between the condition number and the distances to detecting stations. In Fig. 2 the condition number does not have any clear dependency on the distance to the nearest recording station. But Fig. 3 shows a more pronounced dependence on the spread of epicentral distances. As the ratio of the minimum distance to the distance range decreases, the condition number also decreases. These relationships could probably be clarified if events were sorted for those which included

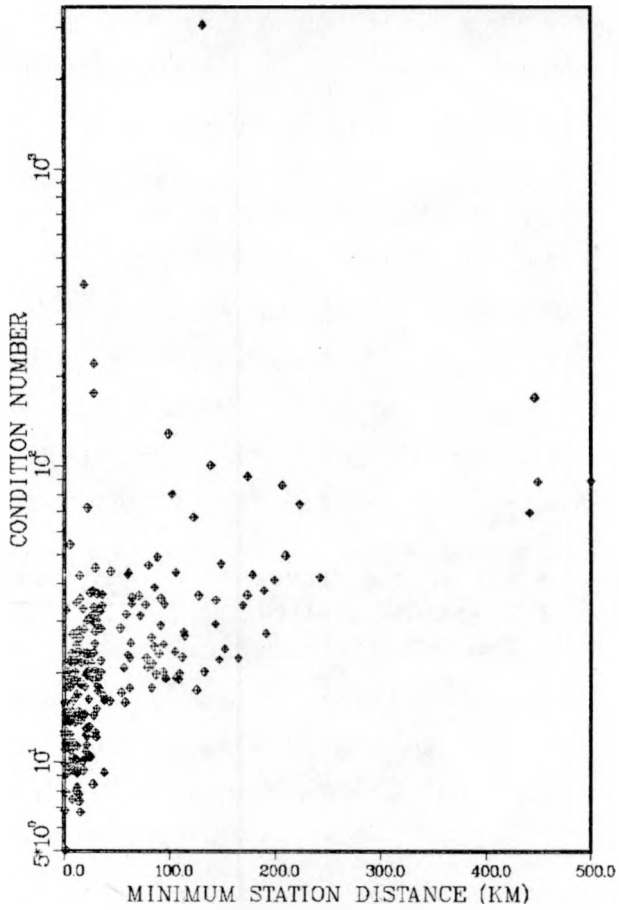

Fig. 2
Condition number of A plotted against distance to the closest recording station.

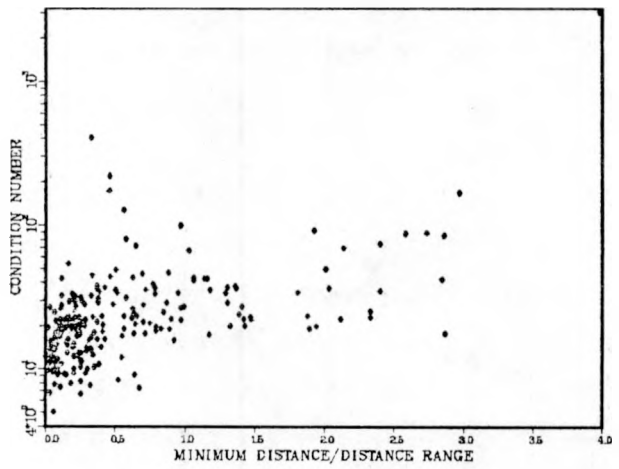

Fig. 3
Condition number of A plotted against the station minimum distance over the distance range for all recording stations.

the focal depth estimation. For most of the data points in these figures, solutions could be obtained only for the origin time and epicentral coordinates.

Figures 4-6 show the RMS residual plotted against the gap, minimum distance, and the condition number, respectively. There is evidently no dependent relationship between the RMS residual and the station gap or the condition number, which illustrates why this parameter should not be used alone to determine the adequacy of the solutions. Distance, as might be anticipated, does effect the RMS residual since arrivals are likely to be more emergent, increasing the picking error.

In Figs. 1 and 4 some large condition number and RMS residual values occur at a gap of 180°. These particular events were located by three to four stations in-line with the epicenter. The maximum azimuthal gap for these cases does not adequately represent the poor station/event geometry. The RMS residual is not always large for the events. But the effect of the poor station configuration is reflected in the high condition numbers.

The method of generalized inversion employed uses a singular value decomposition (SVD) of the A matrix of partial derivatives, or

$$A = U \cdot S \cdot V^T \quad ,$$

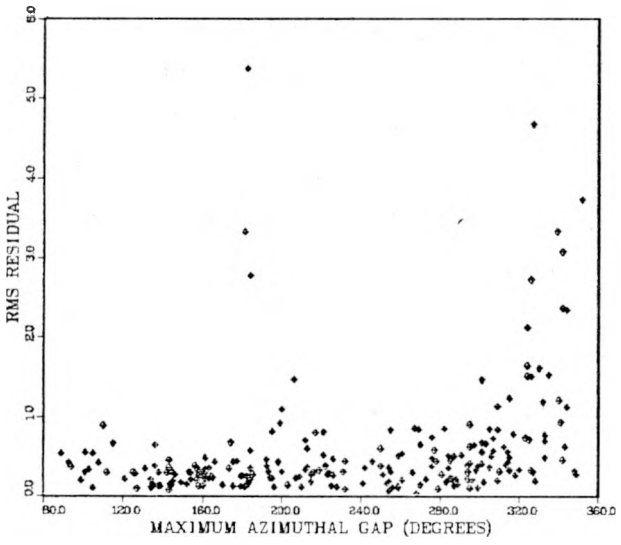

Fig. 4
Root mean square (RMS) of the travel time residuals for 233 events, plotted against maximum azimuthal gap.

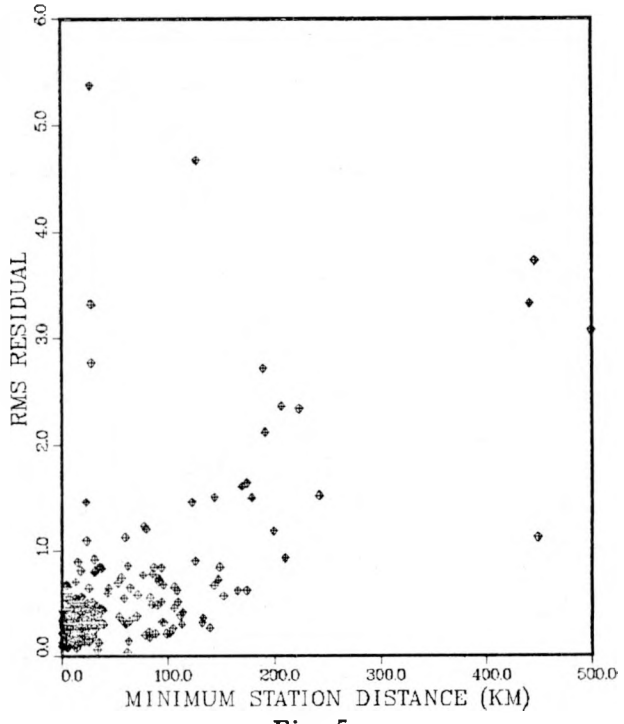

Fig. 5
RMS travel time residual plotted against distance to closest recording station.

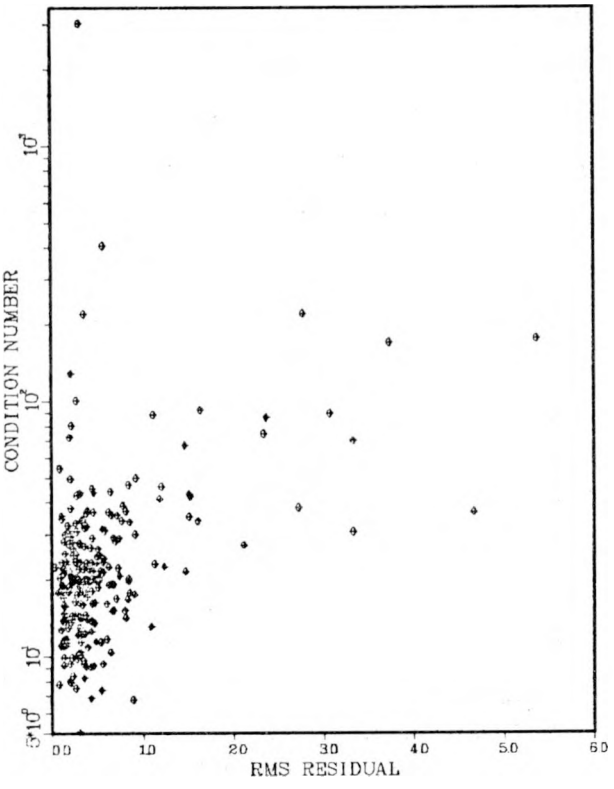

Fig. 6
Condition number of A plotted against the RMS travel time residual.

where V is the matrix of eigenvectors associated with the parameters, U is the matrix associated with the data, and S is the diagonal matrix of eigenvalues. The parameter covariance matrix is then

$$C = w^2 \cdot V \cdot S^{-2} \cdot V^T \quad .$$

In this case w^2 is the variance of the arrival time data, and is computed as the weighted square of the RMS travel time residual. (For a detailed discussion of the weighting scheme see Klein, 1978. Factors include distance, station quality, phase pick quality, and magnitude of residuals.) The error ellipse is then

computed from the 3 x 3 matrix of spatial parameters derived from the covariance matrix (neglecting origin time). Therefore, the three axes of the error ellipse, or the three principal standard errors, are functions of the condition of A and the RMS residual. Figures 7 and 8 show that this is empirically realized, although the exact relationships are not clear. In both cases the lower error values cluster at the lower condition number and RMS values; then as the error values increase, the condition number and RMS values also increase slightly, but with much variation. Other parameters that might affect or otherwise indicate the stability of the solution are plotted in Figs. 9-11. No obvious relationship exists between the condition of A and the number of P arrivals. Increasing condition number (instability) does not increase the number of iterations. But as the number of S-arrivals increases, the condition number seems to decrease, indicating that additional S-phase information can increase the stability of the problem.

An event outside of the seismic array will have a large condition number; the better the array configuration, the smaller the condition number. Figure 12 is a contour map of the condition numbers for 200 earthquakes located throughout northern New Mexico by the Los Alamos array. This map gives a fair indication of the capability of the seismic array with respect to the magnitude and location of most of the northern New Mexico seismic activity. The stations are plotted for reference, but it should be kept in mind that not every station was used for each location. The difference in detection can

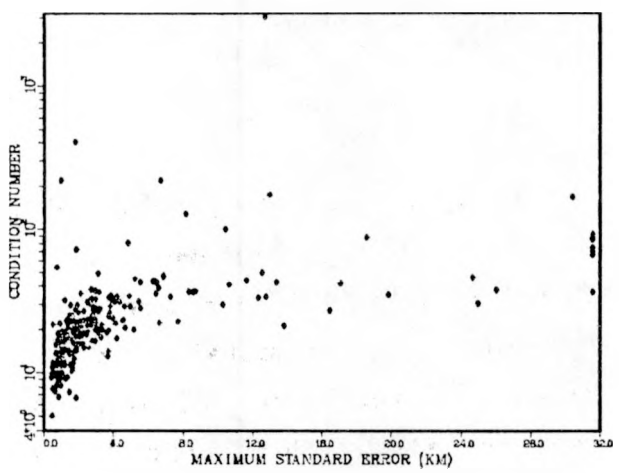

Fig. 7
Condition number of A plotted against the maximum standard error.

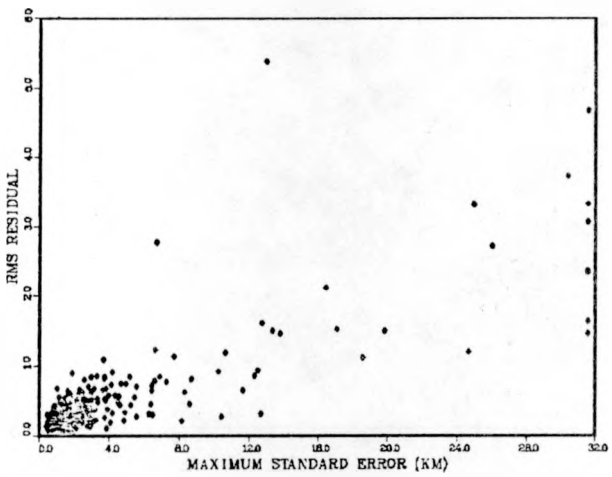

Fig. 8
RMS travel time residual plotted against the maximum standard error.

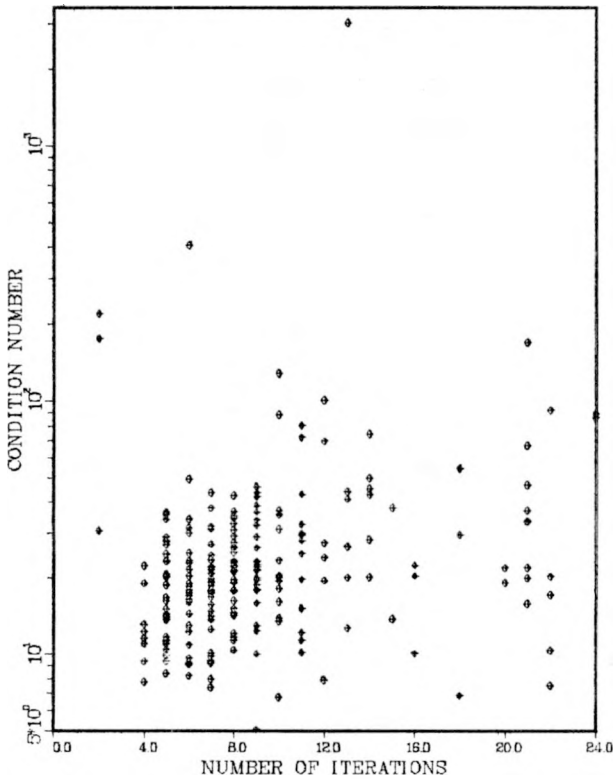

Fig. 9
Condition number of A plotted against the number of iterations for 233 events.

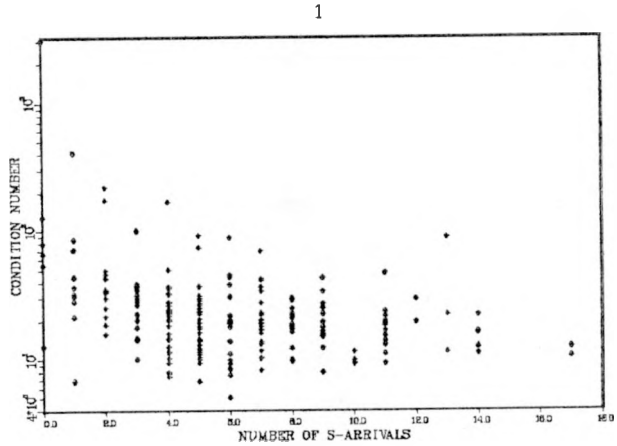

Fig. 11
Condition number of A plotted against the number of S phase arrivals only.

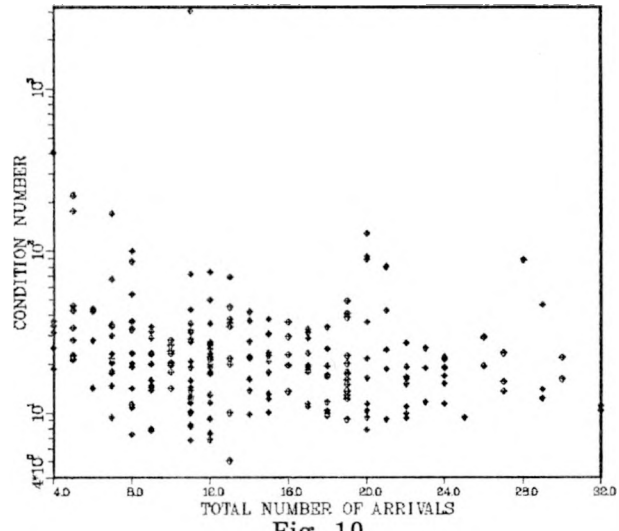

Fig. 10
Condition number of A plotted against the total number of arrivals.

produce a small region with a higher condition number for areas which often have small magnitude events recorded by a limited sub-network of the array.

Because of the additional information supplied by the condition number, the HYPOINVERSE code utilized at Los Alamos has been augmented to assign a quality factor to each hypocenter solution based on the magnitudes of the condition number and the RMS residual. This factor is still qualitative, but does provide an immediate indication of the data adequacy for each event.

C. Termination of the Iteration Procedure

HYPOINVERSE uses an iterative least squares approach to successively minimize the RMS travel-time residual. The method of terminating the

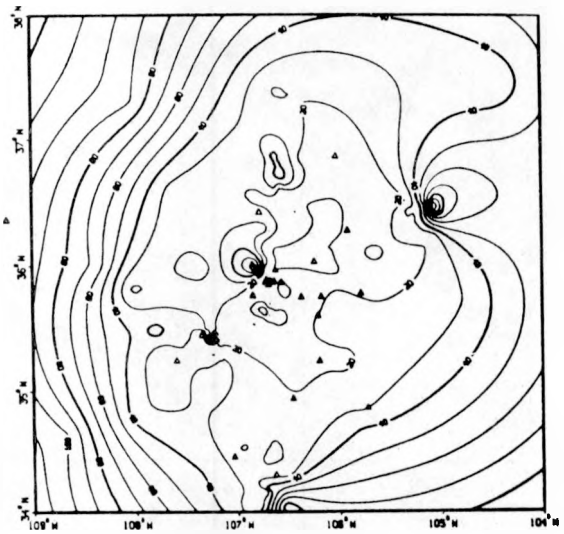

Fig. 12
Contour map of the condition numbers of A for 200 seismic events in northern New Mexico. Contour interval is 10.

iterations is dependent on the desired precision of the solution, and once chosen, convergence criteria can be set low or high depending on the type of data. Iterations in HYPOINVERSE are terminated when the change in the RMS residual becomes smaller than a specified value or when the last step in three-dimensional parameter space (excluding origin time) becomes smaller than a specific value. Convergence almost always occurs before the user-specified maximum number of iterations is reached. However, no test is made to determine whether or not the program has converged to the actual minimum. In the following discussion we will show that often we have only reached a point where the steepness of the RMS contours is small enough to stop the iterations.

III. TESTING CONVERGENCE WITH SYNTHETIC DATA

A. Synthetic Data Generation

To test how well the program could converge to known solutions, empirical results from synthetic data were analyzed. Adaptations to HYPOINVERSE and some additional coding enabled the generation of synthetic data for specified points using any desired combination of velocity models. For northern New Mexico a total of 95 synthetic events were generated with a grid spacing of one-half degree intervals and depths of 5 and 2 km. Each synthetic event has a P-phase and S-phase arrival time computed for every station in the array (Fig. 13). This was done for two arrays; they differed by including in the first array the stations from the Albuquerque Seismological Center (ASC) run by the U.S. Geological Survey (USGS). A similar study was done on a smaller scale for the Jemez Mountains area around Fenton Hill geothermal site. Three sets of synthetic data were generated for this latter study, with 53 synthetic events in each set. The first included all stations within 20 km of the Fenton Hill drill site; the second was the same excluding the five-station

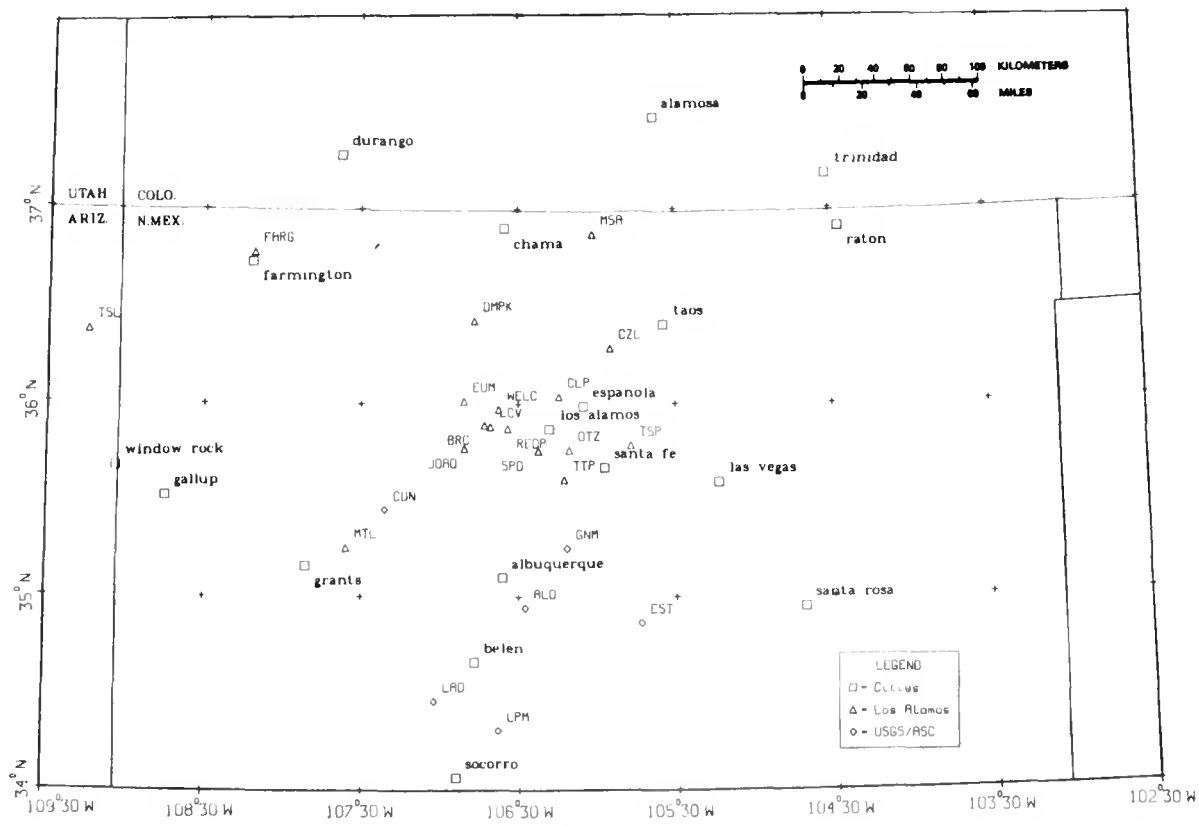

Fig. 13
Seismograph stations in northern New Mexico.

array first deployed by Los Alamos' Q-Division in 1974 (added to the regional telemetered network in 1979), and the third included only those stations within 20 km that were operational before 1979 (see Table I). The latter analysis was divided into three parts to ascertain the relative advantages gained by deploying the more dense station network. Events for the local study near Fenton Hill were computed at depths of 3 km. An option to add random noise to the synthetic data was not used in these studies.

B. Error Computation and Plotting

The synthetic arrival times were run in HYPOINVERSE and solutions were compared to the known hypocenter. The difference between the known hypocenter and the solution, in kilometers, was assigned to each data point. Contour maps were then produced for the grids of mislocation values. The contouring procedure requires two programs. The first generates a regular mesh of values from an irregular set of data points using bivariate interpolation. The second uses contouring and plotting library routines, essentially fitting a

TABLE I

SEISMOGRAPH STATIONS

CODE NAME	GEOGRAPHIC LOCATION	COORDINATES LATITUDE	COORDINATES LONGITUDE	ELEVATION (METERS)	VELOCITY MODEL +	SEISMOMETER	MAGNIFICATION*	TELEMETRY (FREQ.=MHz)	DATE INSTALLED
BRC	Barley Canyon	35.8903	106.7114	2261	2	L4-C	512 K	164.5/LL	20 Nov 75
CLP	Clara Peak	36.0358	106.2403	2591	2	SS-1	240 K	169.0	7 Oct 73
CZL	Cerro Azul	36.2833	105.9103	2128	3	S-13	672 K	410.35	24 Sep 76
DMPK	Dead Man's Peak	36.4264	106.7757	2664	1	S-13	144 K	416.35	22 Nov 76
EUM	Eureka Mesa	36.0131	106.8439	2914	1	L4-3D	216 K	M/226.7	13 Jan 76
FARG**	Farmington	36.7780	108.1870	1801	1	S-500	--		Oct 77
FCN**	Frijoles Canyon	35.7719	106.2503	1945	-	L4-3D	--	LL	7 May 73
JOAQ	Joaquin L.O.	35.7708	106.8411	2768	2	SS-1	720 K	410.35	9 Nov 79
LCV***	La Cueva	35.8828	106.6742	2652	2	L4-3D	456 K	LL	5 Sep 73
LFC	Lake Fork Canyon	35.8769	106.6647	2451	2	Lf-C	288 K	169.0/LL	4 Nov 75
LFMS	Lake Fork Mesa	35.8736	106.7200	2558	2	S-500	576 K	409.075	Nov 79
REDP	Redondo Peak	35.8711	106.5629	3417	2	SS-1	360 K	409.35	Oct 77
LOA**	Los Alamos (TA-49, LANL)	35.8247	106.2944	2144	-	L4-3D	--	LL	12 Jan 72
MSA	San Antonio Mountain	36.8692	106.0216	3322	3	L4-3D	128 K	M/226.7	9 Oct 75
MTL	Mt. Taylor	35.2519	107.5964	3335	1	L4-3D	272 K	M/226.7	15 Oct 75
OTZ	Ortiz Mountain	35.7603	106.1728	2091	3	L4-C	120 K	166.25	17 Sep 76
RIO**	Caja del Rio	35.7547	106.1756	2073	-	L4-C	--	166.25	21 Feb 75
SHMS	Schoolhouse Mesa	35.8544	106.6906	2561	2	S-500	288 K	409.025	Nov 79
SPD	St. Peter's Dome	35.7578	106.3694	2566	2	SS-1	688 K	164.75	18 Sep 73
TMRS	Thompson Ridge	35.8828	106.6375	2476	2	S-500	530 K	409.125	Nov 79
TSL	Navajo Community College	36.3722	109.2436	2012	1	SS-1	344 K	LL	22 May 75
TSP	Tesuque Peak	35.7853	105.7814	3664	2	SS-1	456 K	M/226.7	14 Oct 73
TTP	Tetilla Peak	35.6094	106.2064	2103	3	L4-C	114 K	164.50	18 Mar 75
WELC	Well C Fenton Hill	35.9704	106.6243	2000	2	S-500	512 K	409.	Nov 79
Q-1	Fenton Hill Area	35.8879	106.6716	2658	2	S-13	153 K	M/164.5	Jan 80
Q-2	Fenton Hill Area	35.8783	106.6655	2599	2	S-13	152 K	M/164.5	Jan 80
Q-3	Fenton Hill Area	35.8747	106.6686	2630	2	S-13	152 K	M/164.5	Jan 80
Q-4	Fenton Hill Area	35.8749	106.6793	2634	2	S-13	152 K	M/164.5	Jan 80
Q-5	Fenton Hill Area	35.8787	106.6815	2632	2	S-13	152 K	M/164.5	Jan 80

LL Land Line
M Microwave
* Peak Magnification at 10 Hz
** Closed
*** Fenton Hill site is 300 m south of LCV

S-500 Teledyne-Geotech
L4-C, L4-3D Mark Products
SS-1 Kinemetrics (Ranger)
S-13 Teledyne-Geotech
+ See Table II

surface using a third-order polynomial interpolation between points. The coordinate system on the plots corresponds to latitude and longitude, although no map projection was used. The imprecision is not relevant, since the map only gives a general visual indication of the geometry of the problem.

C. Discussion

Figure 13 shows the distribution of stations in the Los Alamos northern New Mexico seismic array, and Table I gives pertinent information for each station. Velocity model numbers refer to the velocity models listed in Table II. Figure 14 shows locations of the synthetic data. The first series of contour plots (Figs. 15 and 16) are for synthetic data generated for a depth of 5 km. Figures 15a and 15b include the ASC stations, which are not listed in Table I. Figures 15a and 16a show the error in the computed hypocenter; Figs. 15b and 16b are for the epicenter only, meaning that the option to constrain the depth was used during the computation.

Intuitively one would assume that, since the solving of self-generated synthetic data is simply re-working the problem in reverse, the solutions should be exact. However, with an iterative process the method of determining each iterative step and the convergence criteria used are of critical importance. Particularly in the case where an event occurs outside of the array (i.e., with a maximum azimuthal gap of greater than 180°), we can easily

TABLE II

VELOCITY MODELS

APPROXIMATE GEOGRAPHICAL AREA AND REFERENCE	VELOCITY (km/s)	DEPTH (km) TO TOP OF LAYER
1. Colorado Plateau (Roller, 1965)	3.0	0.0
	6.2	2.5
	6.8	27.0
	7.8	45.0
2a. Transition Zone (Toppozada and Sanford, 1976)	3.0	0.0
	6.15	1.0
	6.50	20.0
	7.9	41.0
2b. Jemez Local Seismicity[a]	2.2	0.0
	3.0	0.15
	4.0	0.42
	6.1	0.72
	6.5	5.0
	7.9	41.0
3. Rio Grande Rift (Olsen et al., 1979)	3.33	0.0
	6.0	3.2
	6.4	21.4
	7.6	33.7

[a] Model supplied by Carl A. Newton, Los Alamos National Laboratory.

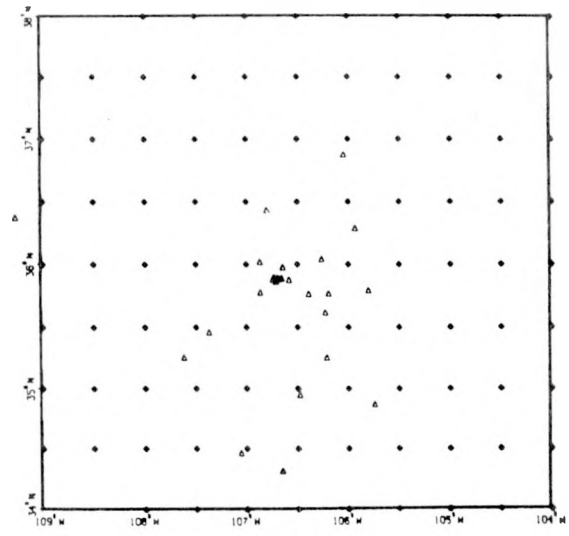

Fig. 14
Positions of synthetic data points for regional array study. Triangles are seismograph stations.

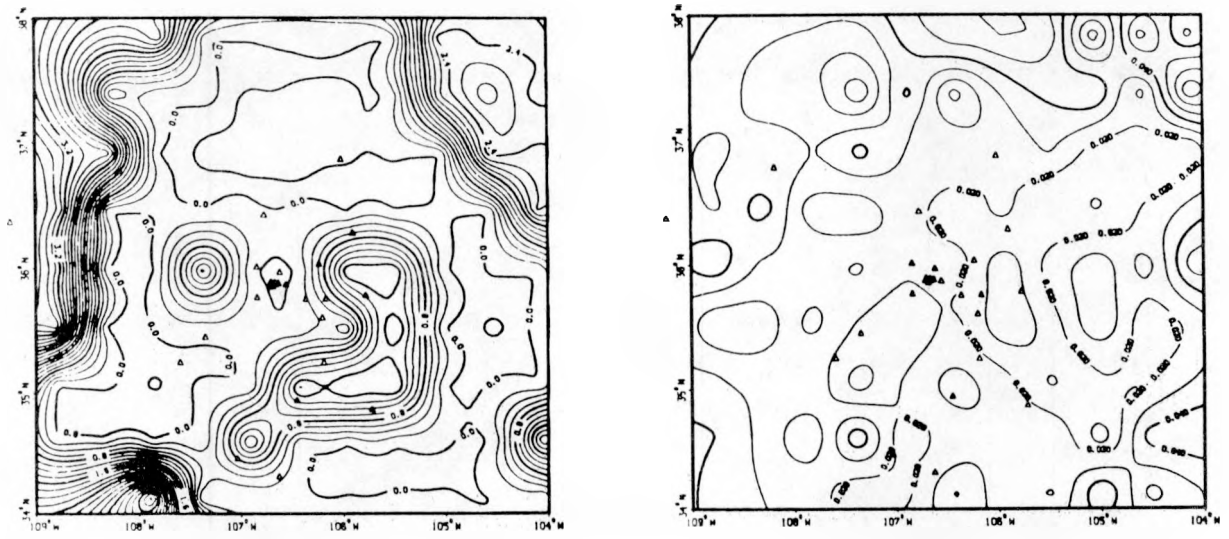

(a) (b)

Fig. 15
Mislocations (km) of synthetic seismic events, Los Alamos and USGS stations. a) Hypocenters, contour interval 0.2 km. b) Epicenters, contour interval 0.01 km.

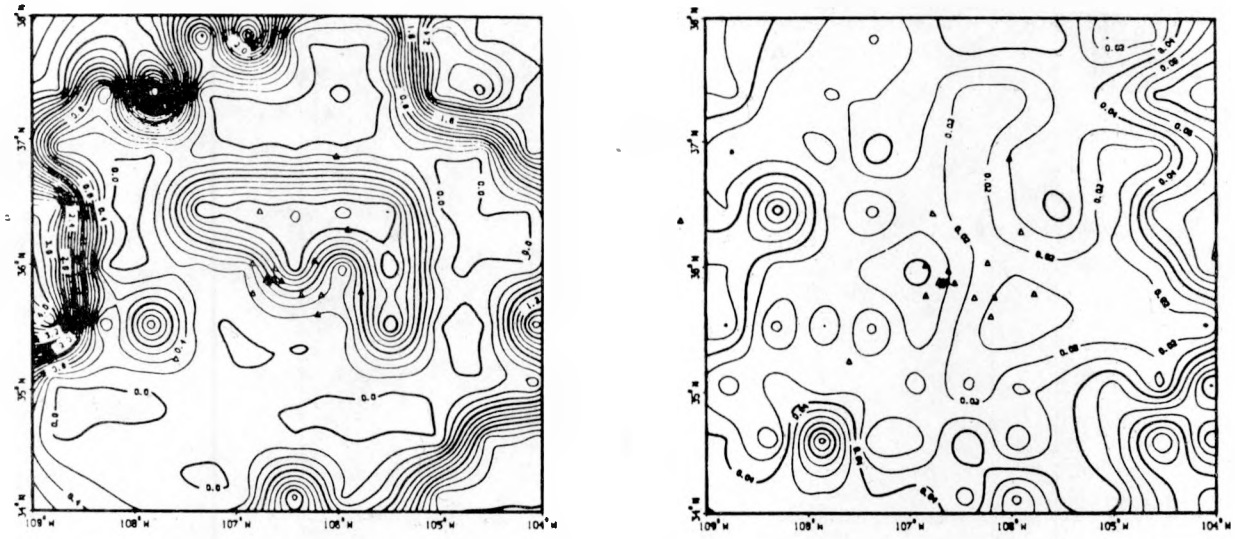

(a) (b)

Fig. 16
Mislocations (km) of synthetic seismic events. Los Alamos stations only. a) Hypocenters, contour interval 0.2 km. b) Epicenters, contour interval 0.01 km.

attain a premature convergence at some relative minimum. In fact, the HYPOINVERSE code does not test for a minimum in the convergence parameters, only a minimum change in parameters, meaning the solution may not even be at a relative minimum. How often this problem occurs and the magnitude of the resultant mislocation turns out to be a function of the array configuration with respect to the epicenter location, as well as the focal depth within the specified velocity model. Comparison of Figs. 15a and 16a with 15b and 16b show that the mislocations are greater and more unpredictable when the depth is not constrained. This is to be expected, since the depth parameter is usually the least well-resolved. But it is clear from the contour plots that the ability to iterate back to the correct locations is not a simple function of epicentral distances.

Further tests also indicate that the focal depth and initial depth for beginning the iteration procedure are important factors in the ability to obtain a solution of the desired precision. Since it is the relative size of the iterative steps that often results in a false or premature convergence, it is very conceivable that approaching the solution from a different direction in four-dimensional parametric space, e.g., using a method of steepest descent, could improve the final estimate. Figure 17 illustrates the differences in the convergence ability that can result when the initial focal depth is set at 9 km, rather than 1 km as for the previous tests. (Recall that the actual depth of these synthetic events is 5 km.) Comparison of this figure with Fig. 15a indicates that in this case approaching the solution from below, rather than above, seems to substantially improve the algorithm's ability to avoid premature convergence.

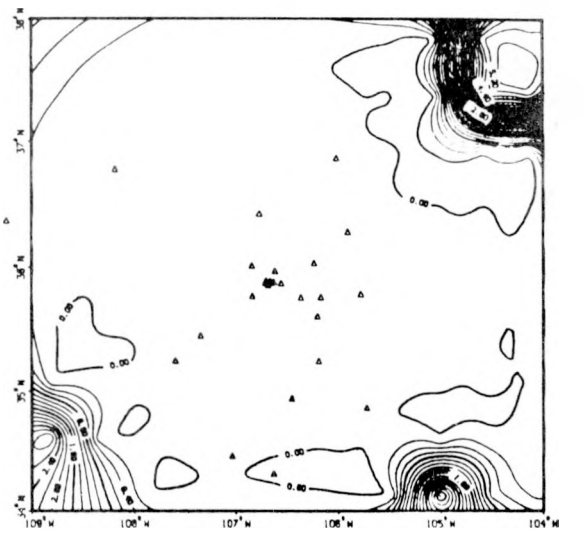

Fig. 17
Mislocations (km) of synthetic events, Los Alamos and USGS stations. Initial depth set at 9 km. Contour interval 0.2 km.

Condition numbers for the synthetic events of the previous figure are contoured in Fig. 18. We observe that there are some general similarities between Figs. 17 and 18, particularly the increases in both

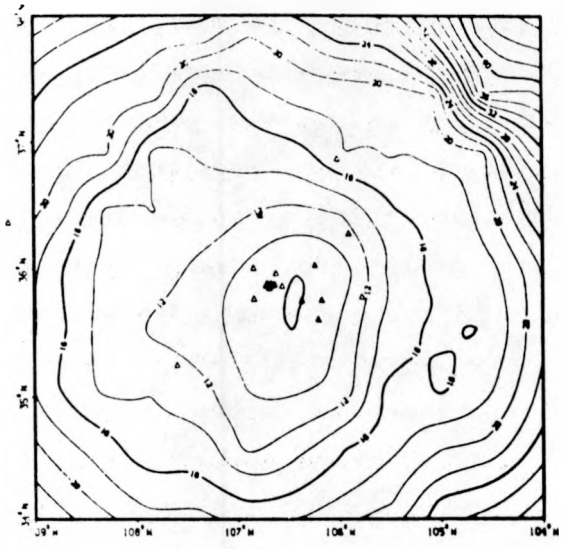

Fig. 18
Condition numbers for synthetic events of Fig. 17. Contour interval is 2.

contour plots toward the edges of the detection area. It should be noted that a direct comparison is not completely valid since the error contours of Fig. 17 are very sensitive to the behavior of the convergence criteria as well as the station distribution. The interesting comparison is between Figs. 12 and 18. Figure 12 shows the irregularities introduced into the contour plot of condition numbers due to the use of real data. The contours of Fig. 12 include the effects of the actual magnitude distribution of northern New Mexico seismic activity, whereas Fig. 18 is the situation that would result if every earthquake were of sufficient magnitude to be equally well recorded at all stations.

A similar study for the Fenton Hill area confirms these conclusions. Figure 19 shows the locations of the seismograph stations, and Fig. 20 depicts synthetic event locations. Figures 21-23 illustrate the successive improvement in the location capability in the Fenton Hill area, as more stations were added in 1978 and 1979. The improvement in depth control is of course considerable. The mislocations are of lesser magnitude and the area of coverage is greatest for the station distribution in Fig. 23.

IV. CONCLUSIONS

A. Evaluating the Location Program

Some conclusions can be drawn about the location algorithm HYPOINVERSE and about location techniques in general. Although the generalized inversion technique gives results that are helpful in determining the quality of hypocenter locations, there remain problems in the interpretation of these results. Comparison of the contour map of the condition number in Fig. 12 with the maps of regions subject to premature convergence in Figs. 15 and 16

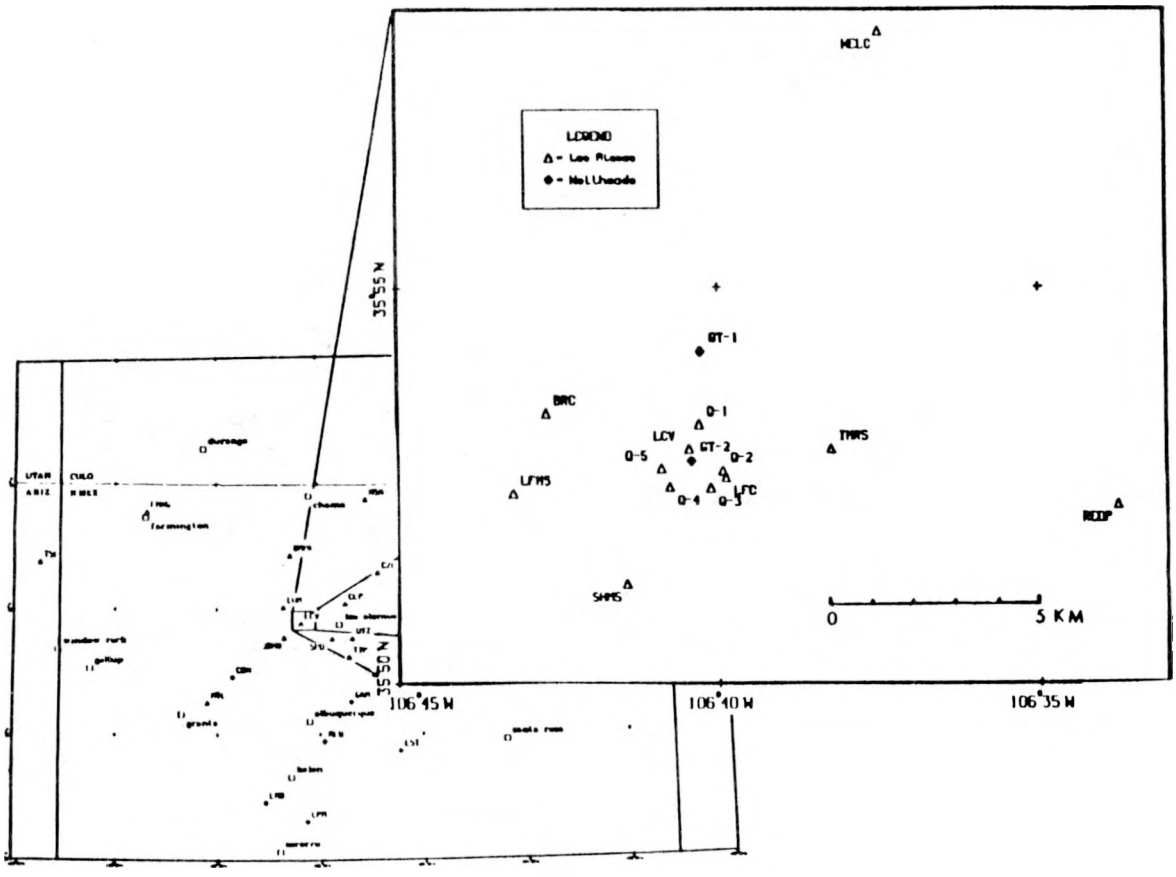

Fig. 19
Seismograph stations in the Fenton Hill, Jemez Mountains, area.

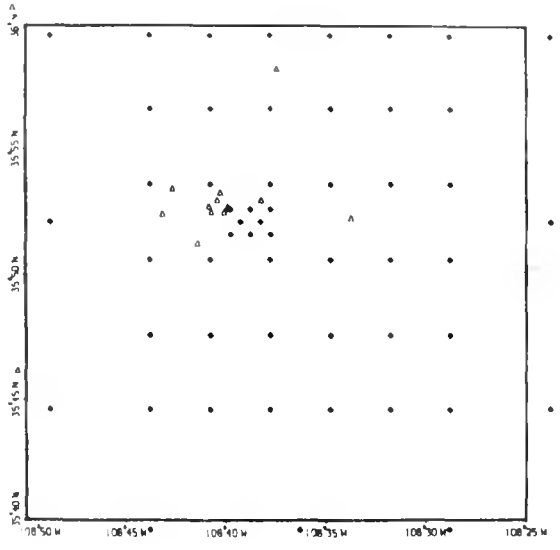

Fig. 20
Positions of synthetic data points for local array study. Triangles are seismograph stations.

gives empirical evidence that the condition of the parameter matrix, which is dependent on data adequacy, can be a measure of the geometrical effects on data adequacy.

Estimating the precision of a hypocenter solution by examining the relative magnitude of the RMS travel-time residual (or the axes of the error ellipse, which are derived from the RMS value) was found to be inadequate. The additional computation of the condition number can lead to more reasonable estimates of the precision, because it takes into

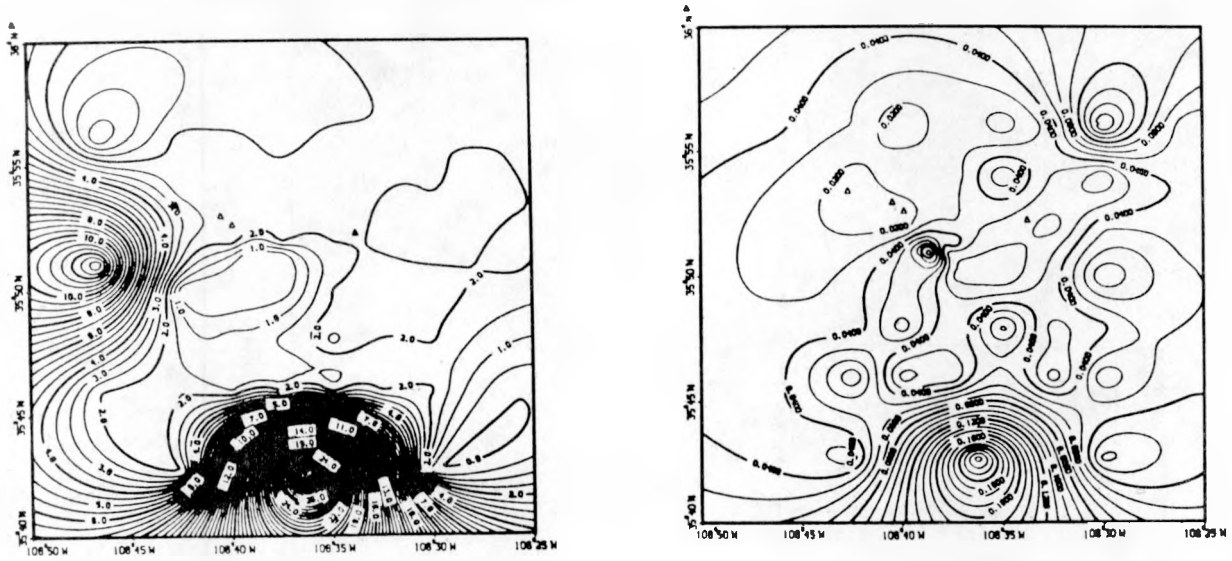

(a) (b)

Fig. 21
Mislocations (km) of synthetic events. Stations used are those which were operational in the area prior to 1979. a) Hypocenters, contour interval 0.2 km. b) Epicenters, contour interval 0.01 km.

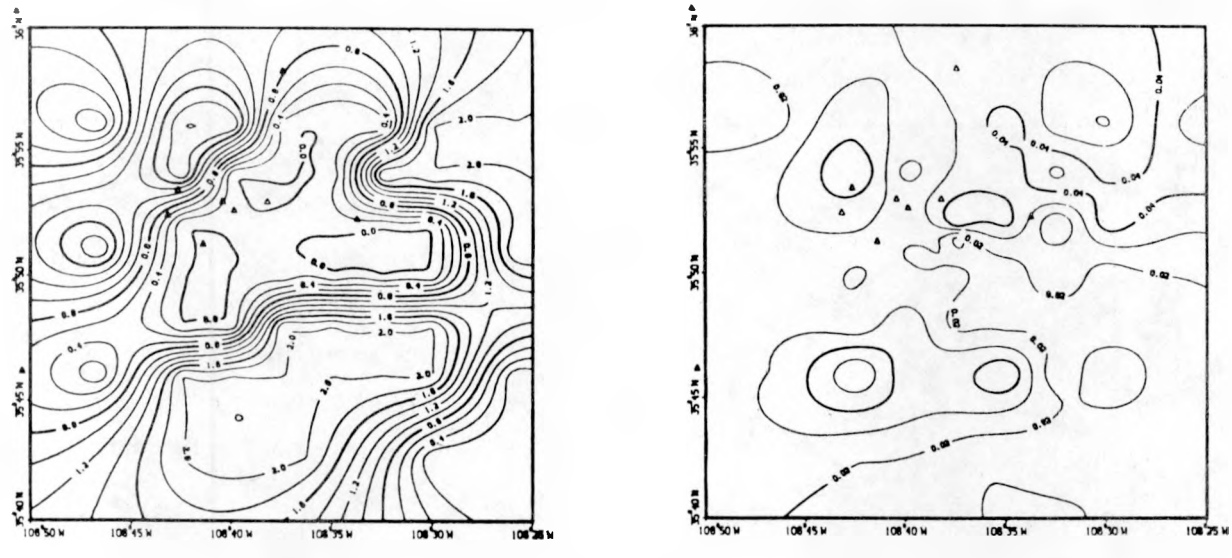

(a) (b)

Fig. 22
Mislocations (km) of synthetic events. Stations used include all within 20 km except the "Q" array (see text). a) Hypocenters, contour interval 0.20 km. b) Epicenters, contour interval 0.01 km.

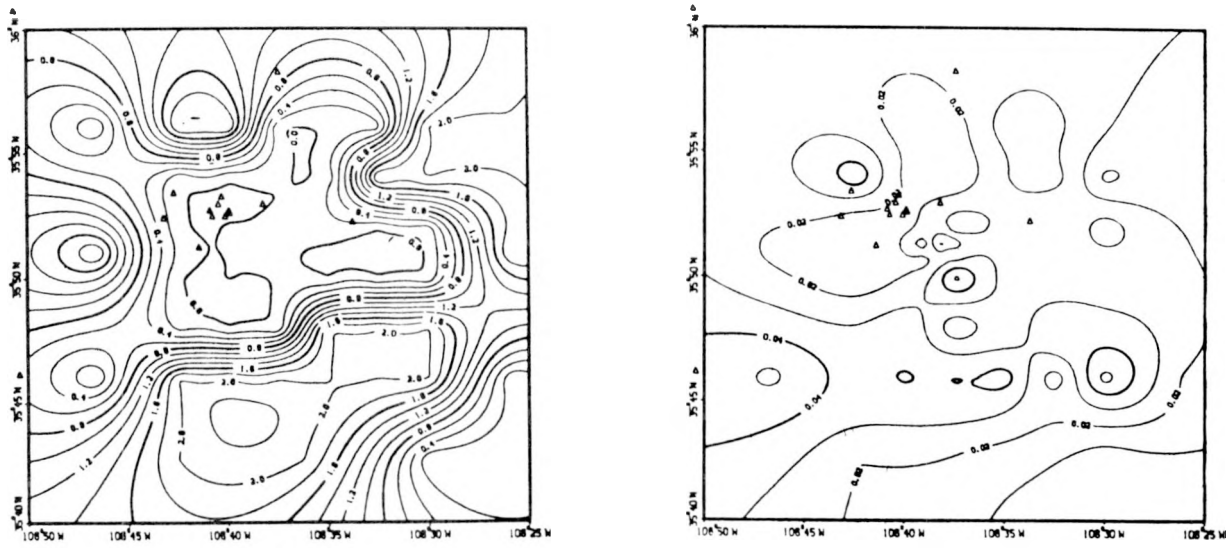

(a) (b)

Fig. 23
Mislocations (km) of synthetic events. Stations used include all those operational in 1980 within 20 km. a) Hypocenters, contour interval 0.20 km. b) Epicenters, contour interval 0.01 km.

account effects of recording array geometry. Using the condition number as a damping factor during the iterative process (a possibility) may prevent solutions which are poorly constrained by the data from completely diverging.

B. Seismicity Distribution

Figure 24 shows the distribution of epicenters located by Los Alamos since 1973. Judging from the contour plots of Figs. 12, 15, and 16, the seismic array is covering the major areas of interest fairly well. For most areas within the -40-contour line of Fig. 12, the precision of locations is probably better than 10 km, and often as good as 1-5 km. The actual precision of an event is very dependent on its magnitude (detectability) and its exact location with respect to the stations recording at that time. It can be seen from Figs. 12 and 22 that the Los Alamos array is adequately providing uniform coverage over an area of relatively high seismicity in the Rio Grande graben of northern New Mexico.

C. Evaluating Station Coverage

How to improve the station coverage in certain areas of interest can be readily assessed by examination of the contour plots of Figs. 21-23. The

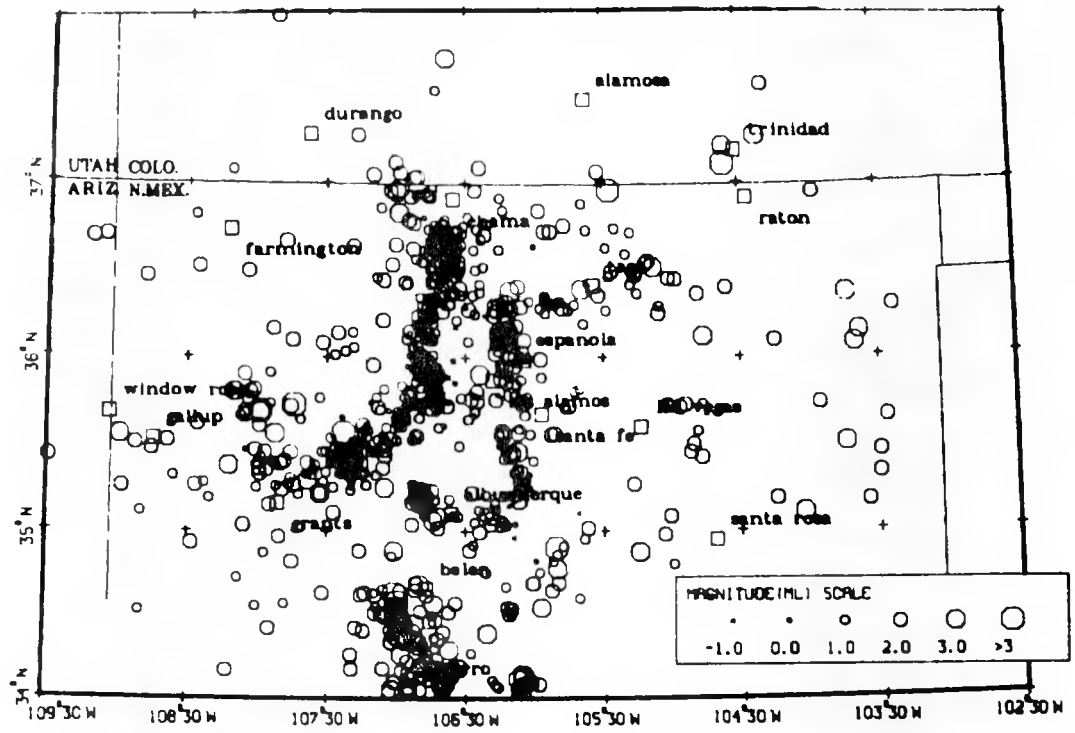

Fig. 24.
Northern New Mexico earthquake epicenters, Sept. 1973 through Sept. 1980.

relative merits of adding more stations to enchance the location capability in areas of interest can be evaluated by noting the areas where the probability of premature convergence and/or condition numbers for events are currently high.

As an example, consider the region of relatively high condition number values at latitude 36°N, longitude 107°W in Fig. 12. This area has a large number of small magnitude events which are detected only by the limited Fenton Hill network, the cluster of stations to the southeast of the high (see also Fig. 19). The condition numbers indicate that the station distribution for this particular area is inadequate. Because the synthetic data of Figs. 15 and 16 employ the entire regional network, they do not show large mislocations in the area. But the error plot contours of the limited Fenton Hill array (Fig. 23) increase toward the northwest. The area of high condition numbers for actual events is just northwest of the region bounded by the plots in Fig. 23. So we have two forms of evidence, the condition numbers of real events and the mislocations of synthetic events, to suggest that station

coverage is insufficient for locating events with magnitudes commonly observed in this area.

Thus, for detailed seismicity studies, we can determine from considerations like the ones just discussed where we need to expand the network to obtain better stability in our hypocentral locations.

ACKNOWLEDGMENTS

Allen Cogbill willingly loaned some of the contouring routines utilized for this study, and discussions with him were helpful. I am grateful for the assistance of J. Stewart and J. Lunsford with various programming considerations. Discussions with M. Harper were beneficial in the development of ideas presented. Finally, I would like to thank Carl Newton for taking the time to review this manuscript.

REFERENCES

1. F. W. Klein, 1978, Hypocenter location program, HYPOINVERSE, U.S. Geological Survey Open-File Report 78-694.

2. K. H. Olsen, G. R. Keller, and J. N. Stewart, 1979, Crustal structure along the Rio Grande Rift from seismic refraction profiles; in Rio Grande Rift: Tectonics and Magmatism, R. E. Riecker, Ed. (American Geophsyical Union, Washington, DC) pp. 127-143.

3. R. C. Roller, 1965, Crustal structure in the eastern Colorado plateau province from seismic-refraction measurements; Bulletin of the Seismological Society of America, v. 55, p. 105.

4. T. R. Toppozada and A. R. Sanford, 1976, Crustal structure in central New Mexico interpreted form the Gasbuggy explosion; Bulletin of the Seismological Society of America, v. 66, p. 877.